

Effects of Structural Distortion Induced by Sc-Substitution in LuFe_2O_4

Jinwon Jeong and Han-Jin Noh*

Department of Physics, Chonnam National University, Gwangju 500-757

Sung Baek Kim

Advancement for College Education Center,

Konyang University, Chungnam, 320-711

(Dated: July 20, 2022)

Abstract

We have studied the correlation between the structural distortion and the electronic/magnetic properties in single crystalline $(\text{Lu,Sc})\text{Fe}_2\text{O}_4$ ($\text{Sc}=0.05$ and 0.3) by using x-ray diffraction (XRD), magnetic susceptibility, and x-ray absorption spectroscopy (XAS)/x-ray magnetic circular dichroism (XMCD). The Rietveld structure analysis of the XRD patterns revealed that the Sc substitution induces an elongation of the FeO_5 bipyramidal cages in LuFe_2O_4 together with the increase of the Fe_2O_4 bilayer thickness. A non-negligible decrease of the ferrimagnetic transition temperature T_C is observed in the magnetic susceptibility curve of the $\text{Sc}=0.3$ sample, but the XAS/XMCD spectra do not show any difference except for a small reduction of dichroism signals at Fe^{3+} absorption edge. We interpret this suppression of T_C as a result of the decreased spin-orbit coupling effect in the Fe^{2+} e_{1g} doublet under D_{3h} symmetry, induced by the weakened structural asymmetry of the FeO_5 bipyramides.

PACS numbers: 75.25.-j, 75.47.Lx, 78.70.Dm

Keywords: LuFe_2O_4 , lattice distortion, spin-orbit coupling

*Electronic address: ffnhj@jnu.ac.kr; Fax: +82-62-530-3369

I. INTRODUCTION

The revived interest in multiferroic systems over the last decade has found various kinds of couplings between multiple long-range orders [1]. One prototypical example for the variety is the ferroelectricity induced by Fe valence ordering in bilayered LuFe_2O_4 [2]. This system has mixed valent Fe cations with one-to-one ratio of divalent and trivalent ions, so the average value of the Fe valences is $\text{Fe}^{2.5+}$. Below ~ 320 K the trivalent ions and the divalent ions are ordered to a specific pattern that breaks an inversion symmetry, inducing ferroelectricity. This ferroelectricity induced by valence ordering is quite contrastive and unique in that the traditional origin of spontaneous electric polarization in solids is so-called d^0 -ness where transition metal cations with no d -electrons are located at an off-centered position [3]. However, the successive studies on this polar state have challenged the originally proposed charge ordered state, and this issue is still under debate [4–9]. Even though it was not definitely determined whether LuFe_2O_4 has a polar state in a macroscopic range, the charge ordered state within an Fe_2O_4 bi-layer is clearly polarized, so the concrete interaction study on the charge and spin orders is still important to understand this system.

A magnetic transition occurs at $T_C \sim 240$ K in this system, so the multiple long range orders i.e. the ferroelectric order and the ferrimagnetic order co-exist below this temperature. The exact spin ordering pattern in the Fe_2O_4 hexagonal bilayer has been proposed by the x-ray absorption spectroscopy (XAS) and x-ray magnetic circular dichroism (XMCD) study [10]. The analysis of the XAS/XMCD spectra suggests that the Fe^{2+} spins are ferromagnetically ordered by the spin-orbit-coupling while the Fe^{3+} spins are antiferromagnetically ordered possibly by the superexchange interaction. The issue on the inter-bilayer magnetic coupling in LuFe_2O_4 is actually coupled to the question whether this system is intrinsically ferroelectric or not [11]. Our previous neutron diffraction study on this issue suggested that the inter-bilayer coupling in LuFe_2O_4 is a mixture of ferromagnetic and antiferromagnetic ones, but ferromagnetic type is preferred [12].

The A-site substitution effects on the Fe spin ordering pattern and on the magnetic transition temperature have been studied in $\text{Lu}_{1-x}\text{L}_x\text{Fe}_2\text{O}_4$ ($\text{L}=\text{Y}$ or Er ; $x=0.1, 0.5$)[12] or in LFe_2O_4 ($\text{L}=\text{Er}$ or Tm) [13]. The partial substitution induces a flattening of the hexagonal unit cell and a frustration of Fe^{3+} spin ordering, but the magnetic transition temperature and the $\sqrt{3} \times \sqrt{3}$ superstructure formation are not affected very much. The full substitution

study also shows the very similar behaviors to those of LuFe_2O_4 except for the indication of extra magnetic phases at a lower temperature than $T_C \sim 240$ K. This is a little bit monotonous result if we want to realize a room temperature multiferroic system other than BiFeO_3 [14]. However, the previous study covers only a partial range of the lattice distortion, i.e. flattening-type distortion of the unit cell, so a complementary study on the effect of lattice elongation has been required to fully understand the exact Fe spin interactions in this class of materials. An experimental investigation toward this complementary direction can be performed by an appropriate choice of substituted cations with a smaller ionic radius than that of the Lu^{3+} ions. In this paper, we focused on the lattice elongation effect in LuFe_2O_4 , and scrutinized a correlation between the electronic/magnetic properties and the lattice distortion by measuring x-ray diffraction (XRD), magnetic susceptibility, XAS, and XMCD for the Sc-substituted LuFe_2O_4 single crystalline samples grown by a floating zone method. The XRD pattern analysis shows that the Sc substitution induces an elongation of the hexagonal unit cell in LuFe_2O_4 together with an elongation of the FeO_5 bipyramidal cages in the Fe_2O_4 bilayers. For Sc=0.3 sample, a discernible amount of decrease (~ 30 K) in magnetic transition temperature was observed in the magnetic susceptibility curve, but no considerable changes in the XAS/XMCD spectra. The decrease of T_C implies that there is correlation between the structural distortion of the Fe_2O_4 bilayers and the Fe^{2+} - Fe^{2+} magnetic interaction strength. We interpret this as a result of the decreased spin-orbit coupling effect in the $\text{Fe}^{2+} 3d e_{1g}$ doublet, which is induced by the weakened structural asymmetry of the FeO_5 bipyramids.

II. EXPERIMENTS

High quality polycrystalline $\text{Lu}_{1-x}\text{Sc}_x\text{Fe}_2\text{O}_4$ ($x=0.05$ and 0.3) was synthesized by the solid state reaction method. Stoichiometric amounts of high purity ($\geq 99.99\%$) dehydrated Lu_2O_3 , Sc_2O_3 , and Fe_3O_4 powders were weighed and mixed with a pestle and mortar. The mixtures were fired two times for feed rods under the flow of CO/CO_2 gas mixture at 1200°C in order to achieve the right oxygen stoichiometry [15]. The single crystals were grown with the feed rods by the floating-zone method using an optical furnace in the laboratory of Pohang Emergent Materials. During the crystal growth process, the flow of CO/CO_2 gas mixture was also maintained at an atmospheric pressure. The single phase of the samples in

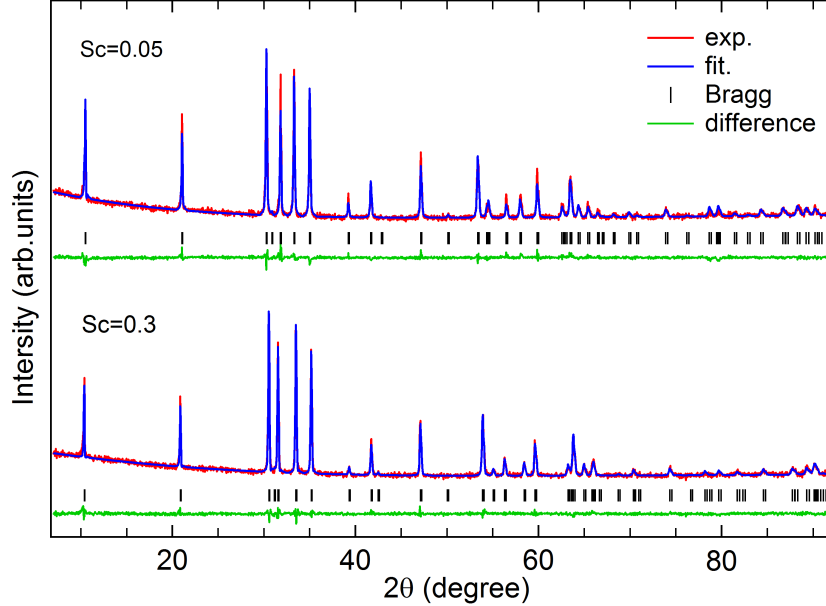


FIG. 1: (Color online) X-ray diffraction patterns of hexagonal bilayered $\text{Lu}_{1-x}\text{Sc}_x\text{Fe}_2\text{O}_4$ ($x=0.05$ and 0.3) at 300 K.

this work was checked by XRD at each step. Magnetization measurements were performed using a commercial magnetometer with a superconducting quantum interference device. The x-ray absorption and x-ray magnetic circular dichroism experiments were performed at the 2A elliptically polarized undulator beam line in the Pohang Light Source. The samples were cleaved *in situ* by the so-called top-post method at the pressure of $\sim 3 \times 10^{-10}$ Torr. The polarization dependent x-ray absorption spectra were obtained at 210 and 300 K, respectively, with $\sim 98\%$ linearly polarized light at 0° and 60° beam incidence to the surface normal. For the XMCD measurements, a 0.6 T magnetic field was applied to the samples to align the magnetic moments at 210 K, and the incident photon angle was 22.5° to the magnetic field direction. The absorption spectra with the energy resolution of ~ 0.15 eV were acquired in a total electron yield mode, and were normalized to the incident photon flux.

III. RESULTS AND DISCUSSION

Figure 1 shows the XRD patterns of our Sc-substituted LuFe_2O_4 with Rietveld analysis results. For each XRD pattern, the blue curve is the fitting profile, the black bars are the

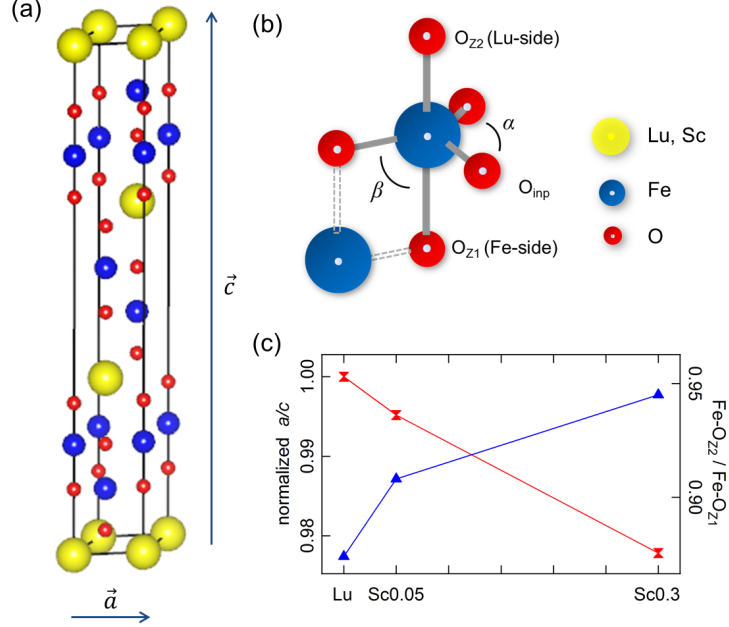
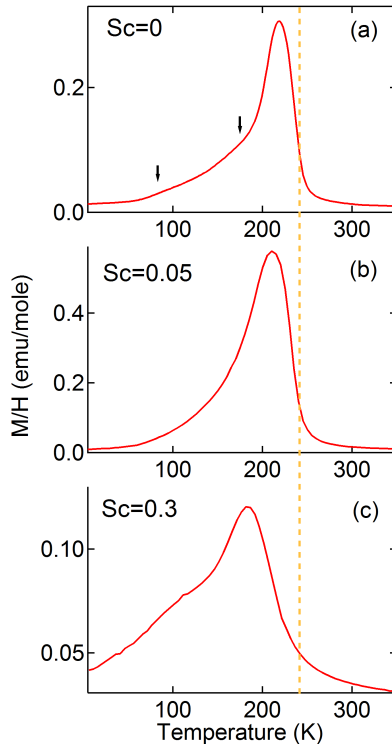


FIG. 2: (Color online) (a) Crystal structure of bilayered LuFe_2O_4 . (b) Bipyramidal FeO_5 cage. (c) Normalized a/c ratio vs. Sc concentration (red sandwatches, left ordinate), and the bond length ratio of Fe-O_{z2} to Fe-O_{z1} (blue triangles, right ordinate).

Bragg peak positions, and the green line is the differences between the observations and fittings, respectively. The two patterns look very similar except for small shifts in peak position, implying that the Sc-substitution induces lattice parameter changes without symmetry changes of the crystal structure. Since the crystal structure of the mother compound LuFe_2O_4 is rhombohedral ($R\bar{3}m$) above the charge ordering temperature ($T_{CO}=320$ K), we refined the crystal structure of Sc-substituted LuFe_2O_4 in the same symmetry using Fullprof [16], mainly focusing on the distortion of FeO_5 bipyramidal cages as a function of Sc concentration. The unit cell of the crystal structure is shown in Fig. 2(a). As the Sc concentration increases, the lattice constant a decreases, but c increases with a small amount of decrease in unit cell volume. In the local structure, the average bond length of Fe-O_{inp} gets shorter but Fe-O_{apical} gets longer, so the FeO_5 bipyramids are elongated. One noticeable thing is that the asymmetry of the bipyramids gets weaker with the increase of Sc substitution. The FeO_5 cages have two kinds of apical oxygen O_{z1} (Fe side) and O_{z2} (Lu side) as shown in Fig. 2(b). The length of Fe-O_{z1} is $\sim 10\%$ longer than that of Fe-O_{z2} in the Sc=0.05 sample, but Fe-O_{z1} is only $\sim 5\%$ longer than that of Fe-O_{z2} together with the $\sim 9\%$ increase of the

TABLE I: Lattice constants and cell parameters for $\text{Lu}_{1-x}\text{Sc}_x\text{Fe}_2\text{O}_4$ ($x=0.05$ and 0.3).

Sc (x)	a ($=b$) [Å]	c [Å]	V [Å ³]	Fe-O _{inp} [Å]	Fe-O _{z1} [Å]	Fe-O _{z2} [Å]	α [deg]	$180^\circ - \beta$ [deg]	χ^2
0.05	3.4318	25.306	258.10	1.996(2)	2.126(18)	1.930(3)	118.51	97.1	2.04
0.3	3.3992	25.508	255.25	1.986(17)	2.233(11)	2.110(2)	117.66	98.9	1.67


 FIG. 3: (Color online) Temperature dependence of the magnetic susceptibility of $\text{Lu}_{1-x}\text{Sc}_x\text{Fe}_2\text{O}_4$ ($x=0.05$ and 0.3).

absolute bond length in the $\text{Sc}=0.3$ sample. The unit cell elongation keeps approximately linear up to $\text{Sc}=0.3$ as shown in Fig. 2(c). In comparison with the bond length change, the major bond angles of O-Fe-O, α and β , change only within $\sim 1\%$ range. Detailed information on the lattice elongation is available in Table I.

Figure 3 shows the magnetic susceptibility curves measured in zero-field-cooled mode under the external field of $H=0.2$ T as a function of sample temperature for Sc-substituted LuFe_2O_4 . From top to bottom, the Sc concentration increases from $\text{Sc}=0.0$ to $\text{Sc}=0.3$, but the susceptibility curves do not show considerable differences in shape. They are quite

similar to that of pristine stoichiometric LuFe_2O_4 reported so far. The magnetization starts to develop at ~ 240 K, reaches its maximum value at ~ 210 K, then decreases down to 4 K. The magnetic transition at $T_C \sim 240$ K is known to be a ferrimagnetic type [10] and to be common in all hexagonal RFe_2O_4 (R=rare-earth metal elements) systems. The clear understanding of the decreasing magnetization below 210 K has not been established yet. The magnitude and the shape of the curve in this temperature range severely depend on the sample preparation conditions and the measuring mode, so several possible scenarios such as the local antiferromagnetic stacking model [17], the collective freezing model [18], and the charge fluctuation model [19], have been proposed, but there is no clear converging view yet. Also, multiple magnetic transitions are reported at ~ 175 , ~ 135 , and ~ 80 K in the oxygen stoichiometric study or the thermal treatment study [17, 18, 20], two of which are barely seen in Fig. 3(a) as indicated by the arrows. Since these low temperature transitions are reported to become prominent for non-stoichiometric samples [21], the shape of our susceptibility curves indicates that the Sc-substituted samples are close to stoichiometric. All our samples but Sc=0.3 show the magnetic transition at $T_C \sim 240$ K. The Sc=0.3 sample shows a considerable lowering of the magnetic transition temperature ($T_C \sim 210$ K). Although the transition temperature is not increased but decreased by Sc-substitution in LuFe_2O_4 , this is a quite noticeable result since the transition temperature in this class of materials is known to be quite robust. Since the Sc substitution induces an elongation of the FeO_5 bipyramids, this implies that the $\text{Fe-O}_{z1/z2}$ length could be the dominant parameter for T_C .

The effects of the Sc substitution on the Fe valence are checked by Fe 2p XAS/XMCD. In Fig. 4 top, the absorption spectra with the photon helicity vector \vec{k} parallel (solid line) and antiparallel (dotted line) to the sample magnetization \vec{M} at Fe L -edge are displayed. Each spectrum shows the spin-orbit split L_3 and L_2 structure at ~ 707 and ~ 719 eV, respectively. In the L_3 structure, two peaks with similar intensity are clearly resolved as designated by Fe^{2+} and Fe^{3+} , which indicates Fe^{2+} and Fe^{3+} ions co-exist with 1:1 ratio in the Sc=0.3 sample. The XAS spectra for the Sc=0.05 sample were not displayed here, but they are statistically identical to that of Sc=0.3 sample. Not only the XAS spectra but also their dichroism signals look quite similar to each other as can be checked in Fig. 4. From bottom to top, the XMCD spectrum for Sc=0.05 (blue) and 0.3 (red) is displayed, respectively. The large downward peak at the Fe^{2+} white line means that the net spin moment of Fe^{2+} ($S=2$) ions is parallel to the applied magnetic field while the small upward peak at the Fe^{3+} white

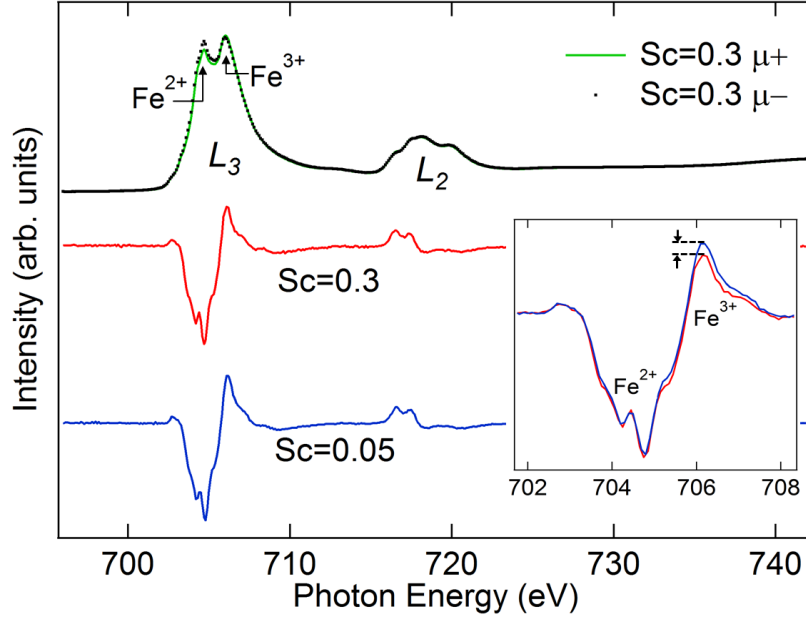


FIG. 4: (Color online) Fe 2p XAS spectra (green/black) of $\text{Lu}_{0.7}\text{Sc}_{0.3}\text{Fe}_2\text{O}_4$ at 210 K, and Fe 2p XMCD spectra of $\text{Lu}_{1-x}\text{Sc}_x\text{Fe}_2\text{O}_4$ ($x=0.05$ (red) and 0.3 (blue)).

line means that the net spin moment of Fe^{3+} ($S=5/2$) is antiparallel to the applied magnetic field. So, the XMCD signal indicates that the Fe spins are ferrimagnetically aligned. Also, the smaller dichroism weight of $S=5/2$ than that of $S=2$ gives a constraint that not all $S=5/2$ spins are aligned parallel to one another. The dichroism peak weight of $S=5/2$ looks almost unaffected by the Sc concentration. In the inset of Fig. 4, we overlap the XMCD spectra to compare the dichroism signals, where only a small reduction of the dichroism peak weight of Fe^{3+} ions for $\text{Sc}=0.3$ is discerned. So, the Sc substitution effects on the Fe^{3+} spin alignment can be regarded negligible. The concrete Fe spin alignment extracted from the XMCD spectra depends on the charge ordering model proposed for this system. If based on the $\sqrt{3} \times \sqrt{3}$ superstructure originally suggested by Ikeda *et al.*, three Fe^{2+} spins and one Fe^{3+} spin are parallel to the sample magnetization vector \vec{M} and two Fe^{3+} spins are antiparallel to \vec{M} [10, 12]. Our XMCD spectra indicate that the magnetic ordering pattern is not affected even though the ferrimagnetic transition temperature is lowered by ~ 30 K in the $\text{Sc}=0.3$ sample.

Figure 5 shows the polarization-dependent O K-edge XAS spectra of each Sc-substituted sample. They commonly show three prominent features in the range of $530 \sim 550$ eV, which correspond to $\text{Fe}^{3+} 3d$, $\text{Fe}^{2+}/\text{Sc}^{3+} 3d$, and $\text{Lu}^{3+} 5d, 6sp/\text{Fe}/\text{Sc} 4sp$ unoccupied states,

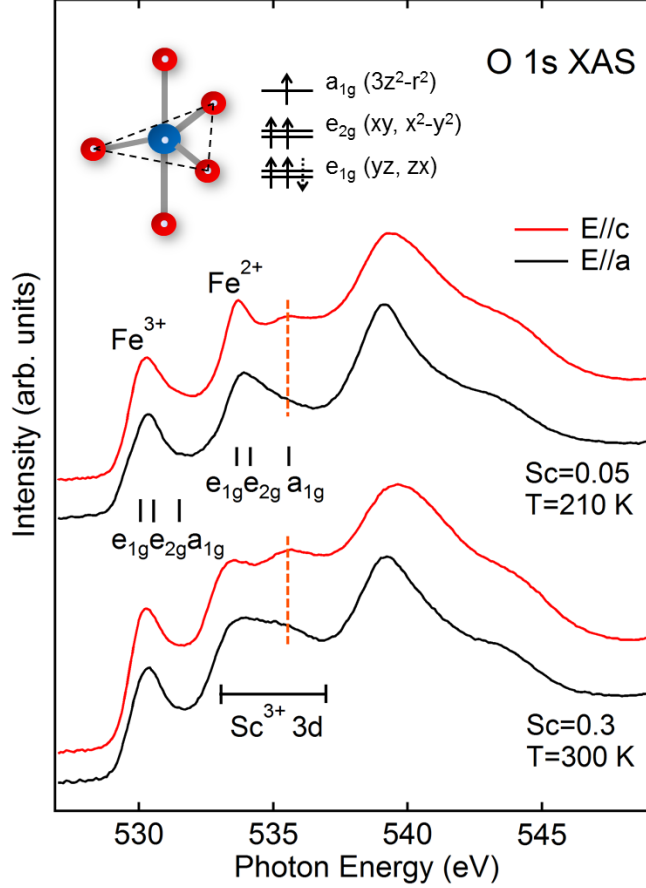


FIG. 5: (Color online) Polarization dependent O K XAS spectra of $\text{Lu}_{1-x}\text{Sc}_x\text{Fe}_2\text{O}_4$ ($x=0.05$ and 0.3). (Inset) schematic diagram of the Fe $3d$ level splittings under bipyramidal crystal electric field.

respectively. As in the case of XAS/XMCD at Fe L -edge, they do not show a prominent dependence on the Sc concentration except for the overlying Sc $3d$ states in the region of the Fe^{2+} $3d$ states (~ 536 eV). Under the crystal electric field produced by a bi-pyramidal FeO_5 cage, the Fe $3d$ states split into two doublets e_{1g} (zx, yz), e_{2g} ($xy, x^2 - y^2$) and one singlet a_{1g} ($3z^2 - r^2$) as shown in the schematic of Fig. 5 [22]. If we consider the dipole selection rule that dominates the absorption process, the O K -edge absorption coefficient for the Fe $3d$ unoccupied states is proportional to the O $2p$ -projected component which is determined by the Fe-O hybridization. The e_{2g} states are hybridized with only in-plane O $2p_{x,y}$ orbitals, while the a_{1g} states mostly with apical oxygen $2p_z$ orbitals. The e_{1g} states are hybridized with both in-plane O $2p_{x,y,z}$ and apical O $2p_{x,y}$. These $2p$ characters in the hybridized Fe $3d$ orbitals are picked up by the photon \vec{E} vector parallel to their orbital directions. Thus, the polarization dependence of the XAS spectra enables us to assign the orbital character

of the Fe^{2+} $3d$ and Fe^{3+} $3d$ structures as indicated in Fig. 5. The assigned orbital energy structure is identical to that of LuFe_2O_4 in the previous study [10].

By combining all our observations, we can deduce one phenomenological result that the increase of the bilayer thickness together with the elongation of the FeO_5 bipyramides in LuFe_2O_4 decreases the ferrimagnetic transition temperature T_C without changing the Fe spin ordering pattern. Since the distance between the inter-layer Fe^{2+} ions gets longer with the increase of the bilayer thickness, the direct exchange coupling between the inter-layer Fe^{2+} ions also weakens, so the decrease of T_C seem to be natural. However, this cannot explain the invariance of the ferrimagnetic transition temperature in RFe_2O_4 (R=rare earth elements) compounds[23]. The experimental data shows that the bilayer thickness does not affect the transition temperature in RFe_2O_4 , which is definitely not parallel to this Sc-substituted LuFe_2O_4 case. More probable scenario is the result of the decreased spin-orbit coupling effect in Fe^{2+} ions. Since the elongation of the structure, the FeO_5 bipyramide becomes less asymmetric as described above. If the crystal electric field in FeO_5 has perfect D_{3h} symmetry, the e_{1g} doublet ($d_{yz/zx} = \frac{i}{\sqrt{2}}(|m_l = 1\rangle + |-1\rangle)/\frac{1}{\sqrt{2}}(|1\rangle - |-1\rangle)$) is truly degenerate. Then, the sixth $3d$ electron in Fe^{2+} ion occupies the $d_{yz/zx}$ states equally, which has no orbital magnetic moment due to the perfect quenching if the spin-orbit coupling in Fe $3d$ states is negligible. In real LuFe_2O_4 system, the spin-orbit coupling plays a key role to the ferromagnetic interaction between the Fe^{2+} ions. However, we note here that the asymmetry of FeO_5 with respect to mirror xy -plane can contribute to the spin-orbit coupling effect. Due to the asymmetry, the e_{1g} state is split with unequal weights of $|m_l = \pm 1\rangle$ components. Usually, this effect is regarded as negligible second order perturbation, but it can be comparable to the spin-orbit coupling of the transition metal $3d$ electrons when the asymmetry is quite large. If LuFe_2O_4 is the case, the polarized $|m_l\rangle$ components in the ground state increase $\langle \vec{L} \cdot \vec{S} \rangle = \langle L_z \cdot S_z \rangle$ (xy -components are isotropic in this case.) as well as the orbital angular momentum. Consequently, the orbital moment quenching competes with the spin-orbit coupling effect. Although the Sc substitution does not recover D_{3h} symmetry perfectly, it reduces the asymmetry in FeO_5 . Then, the increased orbital moment quenching reduces the spin-orbit coupling effect in the Fe^{2+} ions, inducing the weakening of ferromagnetic interaction between the Fe^{2+} ions.

IV. SUMMARY

We successfully synthesized the single crystals of Sc-substituted LuFe_2O_4 for Lu ions by a floating zone method, and investigated the crystal structure distortion and the electronic/magnetic structure change by using XRD, magnetic susceptibility, XAS, and XMCD. The Rietveld structure analysis of the XRD patterns revealed that the Sc substitution induces an elongation of the FeO_5 bipyramidal cages in LuFe_2O_4 together with the elongation of the unit cell. At the concentration of $\text{Sc}=0.3$, a non-negligible decrease of the ferromagnetic transition temperature is observed in the magnetic susceptibility curve, but the XAS/XMCD spectra does not change very much except for a small reduction of dichroism signals at Fe^{3+} absorption edge. The decrease of T_C is quite noticeable since this class of materials is famous for the robust transition temperature at 240 K. We interpret the suppression of T_C as a result of the decreased spin-orbit coupling effect in the $\text{Fe}^{2+} e_{1g}$ doublet under D_{3h} symmetry, induced by the weakened structural asymmetry of the FeO_5 bipyramids in the Sc-substituted LuFe_2O_4 .

Acknowledgments

This work was supported by the National Research Foundation (NRF) of Korea Grant funded by the Korean Government (Grant Nos. 2013R1A1A2058195 and 2010-0010771). The experiments at PLS were supported in part by MSIP and POSTECH.

-
- [1] S.-W. Cheong and M. Mostovoy, *Nature Mater.* 6, 13 (2007).
 - [2] N. Ikeda, H. Ohsumi, K. Ohwada, K. Ishii, T. Inami, K. Kakurai, Y. Murakami, K. Yoshii, S. Mori, Y. Horibe, and H. Kito, *Nature* 436, 1136 (2005).
 - [3] D. I. Khomskii, *J. Magn. Magn. Mater.* 306, 1 (2006).
 - [4] X. S. Xu, J. de Groot, Q.-C. Sun, B. C. Sales, D. Mandrus, M. Angst, A. P. Litvinchuk, and J. L. Musfeldt, *Phys. Rev. B* 82, 014304 (2010).
 - [5] P. Ren, Z. Yang, W. G. Zhu, C. H. A. Huan, and L. Wang, *J. Appl. Phys.* 109, 074109 (2011).
 - [6] J. de Groot, T. Mueller, R. A. Rosenberg, D. J. Keavney, Z. Islam, J.-W. Kim, and M. Angst, *Phys. Rev. Lett.* 108, 187601 (2012).

- [7] D. Niermann, F. Waschkowski, J. de Groot, M. Angst, and J. Hemberger, *Phys. Rev. Lett.* 109, 016405 (2012).
- [8] T. Kambe, Y. Fukada, J. Kano, T. Nagata, H. Okazaki, T. Yokoya, S. Wakimoto, K. Kakurai, and N. Ikeda, *Phys. Rev. Lett.* 110, 117602 (2013).
- [9] J. Lee, S. A. Trugman, C. D. Batista, C. L. Zhang, D. Talbayev, X. S. Xu, S.-W. Cheong, D. A. Yarotski, A. J. Taylor, and R. P. Prasankumar, *Sci. Rep.* 3, 2654 (2013).
- [10] K. T. Ko, H.-J. Noh, J.-Y. Kim, B.-G. Park, J.-H. Park, A. Tanaka, S. B. Kim, C. L. Zhang, and S.-W. Cheong, *Phys. Rev. Lett.* 103, 207202 (2009).
- [11] J. de Groot, K. Marty, M.D. Lumsden, A.D. Christianson, S.E. Nagler, S. Adiga, W.J.H. Borghols, K. Schmalzl, Z. Yamani, S.R. Bland, R. de Souza, U. Staub, W. Schweika, Y. Su, and M. Angst, *Phys. Rev. Lett.* 108, 037206 (2012).
- [12] H.-J. Noh, H. Sung, J. Jeong, J. Jeong, S. B. Kim, J.-Y. Kim, J. Y. Kim, and B. K. Cho, *Phys. Rev. B* 82, 024423 (2010).
- [13] D. H. Kim, J. Hwang, E. Lee, J. Kim, B. W. Lee, H.-K. Lee, J.-Y. Kim, S. W. Han, S. C. Hong, C.-J. Kang, B. I. Min, and J.-S. Kang, *Phys. Rev. B* 87, 184409 (2013).
- [14] S. Lee, W. Ratcliff II, S.-W. Cheong, and V. Kiryukhin, *Appl. Phys. Lett.* 92, 192906 (2008).
- [15] J. Iida, S. takekawa, and N. Kimizuka, *J. Crystal Growth* 102, 398 (1990).
- [16] T. Roisnel and J. Rodriguez-Carvajal, *FullProf*, 2000.
- [17] A. D. Christianson, M. D. Lumsden, M. Angst, Z. Yamani, W. Tian, R. Jin, E. A. Payzant, S. E. Nagler, B. C. Sales, and D. Mandrus, *Phys. Rev. Lett.* 100, 107601 (2008).
- [18] W. Wu, V. Kiryukhin, H.-J. Noh, K.-T. Ko, J.-H. Park, W. Ratcliff, P. A. Sharma, N. Harrison, Y. J. Choi, Y. Horibe, S. Lee, S. Park, H. T. Yi, C. L. Zhang, and S.-W. Cheong, *Phys. Rev. Lett.* 101, 137203 (2008).
- [19] X. S. Xu, M. Angst, T. V. Brinzari, R. P. Hermann, J. L. Musfeldt, A. D. Christianson, D. Mandrus, B. C. Sales, S. McGill, J.-W. Kim, and Z. Islam, *Phys. Rev. Lett.* 101, 227602 (2008).
- [20] S. Patankar, S. K. Pandey, V. R. Reddy, A. Gupta, A. Banerjee, and P. Chaddah, *EPL* 90, 57007 (2010).
- [21] F. Wang, J. Kim, G. D. Gu, Y. Lee, S. Bae, and Y.-J. Kim, *J. Appl. Phys.* 113, 063909 (2013).
- [22] D. Y. Cho, J.-Y. Kim, B.-G. Park, K.-J. Rho, J.-H. Park, H.-J. Noh, B.-J. Kim, S.-J. Oh, H. M. Park, J.-S. Ahn, H. Ishibashi, S.-W. Cheong, J.-H. Lee, P. Murugavel, T.-W. Noh, A.

Tanaka, and T. Jo, Phys. Rev. Lett. 98, 217601 (2007).

[23] N. Kimizuka, A. Takenaka, Y. Sasada, and T. Katsura, Solid State Commun. 15, 1321 (1974).